# Supplementary Material for: "The predictability barrier of climate instabilities"

Nina Doerfler,[1,2,3] Anders Levermann[1,2,3*]

[1]Potsdam Institute for Climate Impact Research, Potsdam, Germany
[2]Max-Planck Institute of Geoanthropology, Jena, Germany
[3]Institute for Physics and Astronomy, Potsdam University, Potsdam, Germany

*Corresponding author; E-mail: anders.levermann@pik-potsdam.de

## Supplementary Note 1: Generic saddle-node bifurcation in tipping elements

The concept of a climate "tipping element" was introduced by Lenton et al. 2008 [1] to describe subsystems of the Earth system in which a small change in forcing can trigger a disproportionately large, qualitative and often hard-to-reverse change of state, driven by an internal self-amplifying feedback. This original definition is phenomenological: a tipping point is characterised by the outcome of crossing it – an abrupt, persistent reorganisation of the system – rather than by a criterion on the system's own internal dynamics.

A more dynamical definition was subsequently proposed by Levermann et al. 2012 [2]: a system possesses a tipping point only if it contains an internal positive feedback strong enough that, once triggered, it *dominates* the system's own dynamics until it has reached a qualitatively different state. (This definition was later adapted by Armstrong-McKay et al. 2022 [3]). In dynamical-systems terms this is an instability criterion: the local growth rate of a perturbation turns positive and the previously restoring branch of the dynamics becomes locally unstable. In the notation of the main text this is exactly the condition $\partial_x f = 0$ changing sign at the critical point $(x_c, \theta_c)$ (Eq. (10)), and it underlies the distinction drawn in the main text between the tipping temperature, the tipping point and the point of no return.

Self-amplifying feedbacks of this kind have since been identified and formalised, through dedicated conceptual or reduced-order process models, for essentially every climate subsystem commonly discussed as a tipping element. These models fall into two structural classes, depending on whether, at the critical point, the old equilibrium merges onto a single remaining branch (a bare saddle-node, with no nearby second attractor) or onto a genuine second stable

state (the double-fold, cusp-catastrophe structure that the normal form of Eq. (6) generalises). Table S1 lists representative examples of both classes.

| **Tipping element** | **Conceptual model** | **Normal form** |
|---|---|---|
| Atlantic meridional overturning circulation | Two-box salt-advection model [4] | Saddle-node |
| Atlantic subpolar gyre | Bistability mechanism [5]; four-box conceptual model [6] | Saddle-node |
| Indian summer monsoon | Moisture-advection box model [7] | Saddle-node |
| Sahara/Sahel vegetation | Vegetation–atmosphere box model [8] | Saddle-node |
| West Antarctic ice sheet | Boundary-layer grounding-line theory [9, 10] | Saddle-node |
| Arctic sea ice (annual-mean) | Small ice-cap instability [11] – fold removed once a seasonal cycle is included [12] | Saddle-node |
| Greenland ice sheet | Melt–elevation feedback [13], consistent with numerically found multistability [14] | Cusp (two folds) |
| Amazon rainforest / savanna | Fire–tree-cover feedback [15] | Cusp (two folds) |
| Boreal forest/tundra | Tree-cover transition analysis [16] | Multiple folds (beyond a single cusp) |
| Antarctic ice sheet (full) | Coupled ice-sheet/climate hysteresis [17] | Multiple folds (beyond a single cusp) |

Not every proposed climate tipping element reduces to a fold of this kind. Most notably, the El Niño–Southern Oscillation's own conceptual model, the recharge oscillator [18], undergoes a Hopf bifurcation – an instability of a qualitatively different kind, producing a self-sustained oscillation rather than a jump between two fixed states. A formal classification distinguishing such cases (bifurcation-, noise-, and rate-induced tipping) is given Ashwin et al. 2012 [19]. The analysis in the present paper is restricted to the fold/cusp class, for which the double-fold normal form of Eq. (6) is, as Table S1 illustrates, both a mechanistically motivated and broadly applicable reduction: it contains the bare saddle-node as the local behaviour near either of its two folds (cf. Supplementary Note 2), while also accommodating systems that land on a genuine second stable state.

## Supplementary Note 2: Scaling laws near critical point

Throughout the paper we illustrate the results using the generic cubic normal form of the cusp catastrophe, whose fold (saddle-node) bifurcations we study. In order to be able to compare orders of magnitude of the different time scales involved we start with a slightly more general

dimensional form of the normal form, namely

$$\frac{d}{dt}x = \frac{x_0}{2\tau_s}\left(-\left(\frac{x}{x_0}\right)^3 + \left(\frac{x}{x_0}\right) + \theta\right) \equiv f(x,\theta). \tag{S1}$$

where $x_0$ is a scale that will drop out of practically all results, while $\tau_s$ is the time scale parameter of the system and $\theta$ is the non-dimensional control parameter.

Since we are interested in the time scaling of the trajectory close to the fold, we expand around the critical point and forcing $(x_c, \theta_c)$, where $\delta x = x - x_c$

$$\dot{\delta x} = f(x_c,\theta_c) + \left.\frac{\partial f}{\partial x}\right|_{(x_c,\theta_c)} \delta x + \left.\frac{\partial f}{\partial \theta}\right|_{(x_c,\theta_c)} (\theta - \theta_c) + \frac{1}{2}\left.\frac{\partial^2 f}{\partial x^2}\right|_{(x_c,\theta_c)} (\delta x)^2 + \mathcal{O}(\delta x^3) \tag{S2}$$

$$= \frac{x_0}{2\tau_s}\left[-\frac{3x_c}{x_0^3}(\delta x)^2 + (\theta - \theta_c)\right] \tag{S3}$$

Without loss of generality we choose a positive $x_0$ and consider cases of $\theta > 0$. Since we initialise the system in $x(0)/x_0 = -1$, we use $x_c/x_0 = -1/\sqrt{3}$ and $\theta_c = 2/(3\sqrt{3})$. Setting $\theta - \theta_c = (t - t_c)/\tau_f$ where $\tau_f$ is the time scale of the forcing we get

$$\frac{2\tau_s}{x_0}\dot{\delta x} = -\frac{3x_c}{x_0^3}(\delta x)^2 + \frac{t - t_c}{\tau_f}. \tag{S4}$$

To non-dimensionalise the system we introduce two so-far undetermined scales $X_{scale}$ and $T_{scale}$ and define the non-dimensional variables

$$\tilde{x} = \frac{\delta x}{X_{scale}} \qquad\qquad \tilde{t} = \frac{t - t_c}{T_{scale}}. \tag{S5}$$

The derivative is then

$$\frac{d\delta x}{dt} = \frac{d\delta x}{d\tilde{x}}\frac{d\tilde{x}}{d\tilde{t}}\frac{d\tilde{t}}{dt} = \frac{X_{scale}}{T_{scale}}\frac{d\tilde{x}}{d\tilde{t}}. \tag{S6}$$

Transforming Eq. (S4) wrt. the dimensionless coordinates then gives us

$$\frac{2\tau_s}{x_0}\frac{X_{scale}}{T_{scale}}\frac{d\tilde{x}}{d\tilde{t}} = -\frac{3x_c}{x_0^3}X_{scale}^2\tilde{x}^2 + \frac{\tilde{t}T_{scale}}{\tau_f}. \tag{S7}$$

Dividing through yields

$$\frac{d\tilde{x}}{d\tilde{t}} = -\frac{3x_c}{2\tau_s x_0^2}\cdot X_{scale}T_{scale}\cdot\tilde{x}^2 + \frac{x_0}{2\tau_s\tau_f}\frac{T_{scale}^2}{X_{scale}}\cdot\tilde{t}. \tag{S8}$$

In order to get the dimensionless equation

$$\frac{d\tilde{x}}{d\tilde{t}} = \tilde{x}^2 + \tilde{t} \tag{S9}$$

we can now choose the constants such that they eliminate all parameters from the equation. For this we solve the equations

$$X_{scale}T_{scale} = -\frac{2\tau_s x_0^2}{3x_c} \tag{S10}$$

$$\frac{T_{scale}^2}{X_{scale}} = \frac{2\tau_s\tau_f}{x_0} \tag{S11}$$

by

$$T_{scale} = \left(\frac{4}{3}\frac{x_0}{x_c}\tau_f\tau_s^2\right)^{1/3} = \left(\frac{4\sqrt{3}}{3}\tau_f\tau_s^2\right)^{1/3} \sim \tau_f^{1/3}\tau_s^{2/3} \tag{S12}$$

$$X_{scale} = \frac{x_0}{2\tau_s\tau_f}T_{scale}^2 = \left(\frac{2}{9}\cdot\frac{\tau_s}{\tau_f}\cdot\left(\frac{x_0}{x_c}\right)^2\right)^{1/3} x_0 = x_0\left(\frac{2}{3}\frac{\tau_s}{\tau_f}\right)^{1/3} \sim \frac{\tau_s^{1/3}}{\tau_f^{1/3}} \tag{S13}$$

This means that for any given system all time differences around the critical point scale with $\tau_f^{1/3}\tau_s^{2/3}$ while any state differences scale as $\tau_f^{-1/3}\tau_s^{1/3}$. The slope of the transition scales like

$$\frac{X_{scale}}{T_{scale}} \sim \frac{\tau_f^{-1/3}\tau_s^{1/3}}{\tau_f^{1/3}\tau_s^{2/3}} = \tau_f^{-2/3}\tau_s^{-1/3}. \tag{S14}$$

## Supplementary Note 3: Analytic calculation of the ensemble variance

In order to get an expression for the variance along the whole trajectory we again linearise the system, this time around the deterministic solution $x_{det}$.

### 3.1 White noise

For simplicity, we start by using white noise. In section 3.2 we will expand the derivation to include red noise instead. For now, setting $x(t) = x_{det}(t) + \delta x(t)$ and naming the noise intensity $g$, we get

$$\frac{dx}{dt} = \frac{d(x_{det}+\delta x)}{dt} = \frac{1}{2\tau_s}f(x_{det}+\delta x,\theta) + g\eta(t) \tag{S15}$$

$$\dot{x}_{det} + \dot{\delta x} = \left[\frac{1}{2\tau_s}f(x_{det},\theta) + \frac{1}{2\tau_s}\partial_x f(x_{det},\theta)\delta x + \mathcal{O}(\delta x^2)\right] + g\eta(t). \tag{S16}$$

For now we only keep the linear term. Since $\dot{x}_{det} = \frac{1}{2\tau_s} f(x_{det}, \theta)$ we are left with

$$\frac{d\delta x}{dt} = \frac{1}{2\tau_s}(1 - 3x_{det}^2)\delta x + g\eta(t) = \lambda(t)\delta x + g\eta(t) \tag{S17}$$

$$d\delta x = \frac{1}{2\tau_s}(1 - 3x_{det}^2)\delta x dt + g dW_t = \lambda(t)\delta x dt + g dW_t \tag{S18}$$

where we defined the local growth rate (restoring rate) $\lambda(t) = \frac{1}{2\tau_s}(1 - 3x_{det}^2)$. Then

$$d(\delta x^2) = 2\delta x d\delta x + (d\delta x)^2. \tag{S19}$$

Inserting the equation for $d(\delta x)$ and only keeping terms up to linear order in $dt$ we get

$$d(\delta x^2) = 2\lambda(t)\delta x^2 dt + g^2 dt + 2\delta x g dW_t. \tag{S20}$$

Taking the expectation value of this equation, since for white noise $\mathrm{E}[2\delta x g dW_t] = 0$ we are left with the linear variance equation

$$\frac{dV}{dt} = \frac{1}{\tau_s}(1 - 3x_{det}^2)V + g^2 = 2\lambda(t)V + g^2. \tag{S21}$$

The physical meaning of this equation is explained in more detail in the Methods and the main text. We can compute the equilibrium variance by setting the right-hand side to zero

$$V_{equ} = -\frac{g^2}{2\lambda} = \frac{g^2\tau_s}{3x_{det}^2 - 1}. \tag{S22}$$

This solution has a pole at the critical point $x_{det} = x_c$. Note that this does not mean that generally speaking, variance peaks at $x_c$. Rather it means that the system is strongly out of equilibrium and the closer we move to the critical point, the more the equilibrium approximation breaks down. It is thus useful to fully solve the variance equation Eq. (S21). Since it is a linear, first order, inhomogeneous ODE, we can solve it with an integrating factor

$$\mu(t) = e^{-\int_{t_0}^{t} 2\lambda(u)du} \qquad \text{such that} \qquad \dot{\mu} = -2\lambda\mu. \tag{S23}$$

Multiplying through by $\mu$, we can use the inverse chain rule to write

$$\frac{d}{dt}(\mu V) = \mu g^2 \tag{S24}$$

which can now easily be integrated yielding

$$\mu(t)V(t) - \mu(t_0)V(t_0) = \int_{t_0}^{t} \mu(s)g^2 ds \tag{S25}$$

$$\Leftrightarrow V(t) = \frac{1}{\mu(t)}V(t_0) + \frac{g^2}{\mu(t)}\int_{t_0}^{t} \mu(s)ds. \tag{S26}$$

Inserting for $\mu$ we obtain the solution

$$V(t) = V(t_0)e^{\int_{t_0}^{t} 2\lambda(u)du} + g^2 \int_{t_0}^{t} e^{\int_{s}^{t} 2\lambda(u)du} ds. \tag{S27}$$

## 3.2 Red noise

Since red noise has its own time scale and evolution, we now have two coupled differential equations

$$\frac{dx}{dt} = \frac{1}{2\tau_s}\left(-x^3 + x + \theta(t)\right) + \xi(t) \tag{S28}$$

$$\frac{d\xi}{dt} = -\frac{1}{\tau_n}\xi + \sqrt{\frac{2\sigma^2}{\tau_n}}\eta(t) \tag{S29}$$

where $\tau_n$ is the correlation time of the noise, $\eta(t)$ is white noise and $\sigma$ is the stationary variance of $\xi$

$$\langle \xi^2 \rangle_* = \sigma^2. \tag{S30}$$

We again define

$$\lambda(t) = \frac{1 - 3x_{det}^2}{2\tau_s} \tag{S31}$$

as the relaxation rate of the system. After expanding around $x_{det}$ and keeping only the linear order we get

$$\frac{d(\delta x)}{dt} = \lambda \delta x + \xi \tag{S32}$$

$$\frac{d\xi}{dt} = -\frac{1}{\tau_n}\xi + \sqrt{\frac{2\sigma^2}{\tau_n}}\eta(t). \tag{S33}$$

We can write this as a matrix multiplication

$$\frac{d}{dt}\begin{pmatrix}\delta x \\ \xi\end{pmatrix} = \begin{pmatrix}\lambda & 1 \\ 0 & -1/\tau_n\end{pmatrix}\begin{pmatrix}\delta x \\ \xi\end{pmatrix} + \begin{pmatrix}0 \\ \sqrt{\frac{2\sigma^2}{\tau_n}}\eta\end{pmatrix} \tag{S34}$$

$$\frac{d}{dt}\mathbf{y} = \mathbf{J}(t)\mathbf{y} + \eta\mathbf{b}. \tag{S35}$$

The covariance matrix of $\mathbf{y}$ is

$$\Sigma(t) = \langle \mathbf{y}\mathbf{y}^T \rangle = \begin{pmatrix}\langle \delta x^2 \rangle & \langle \delta x \xi \rangle \\ \langle \xi \delta x \rangle & \langle \xi^2 \rangle\end{pmatrix}. \tag{S36}$$

Then the time evolution is

$$\dot{\Sigma}(t) = \langle \dot{\mathbf{y}}\mathbf{y}^T \rangle + \langle \mathbf{y}\dot{\mathbf{y}}^T \rangle = \langle (\mathbf{J}\mathbf{y} + \mathbf{b}\eta)\mathbf{y}^T \rangle + \langle \mathbf{y}(\mathbf{y}^T\mathbf{J}^T + \eta\mathbf{b}^T) \rangle \tag{S37}$$

$$= \mathbf{J}\Sigma + \Sigma\mathbf{J}^T + \mathbf{Q} \tag{S38}$$

where we defined

$$\langle \eta\mathbf{b}\mathbf{y}^T \rangle + \langle \eta\mathbf{y}\mathbf{b}^T \rangle = \mathbf{b}\mathbf{b}^T \equiv \mathbf{Q}. \tag{S39}$$

After performing the matrix multiplication in Eq. (S34) we get the following three differential equations for the time evolution of the matrix elements

$$\langle \dot{\delta x^2} \rangle = 2\lambda \langle \delta x^2 \rangle + 2\langle \delta x \xi \rangle \tag{S40}$$

$$\langle \dot{\delta x \xi} \rangle = \left( \lambda - \frac{1}{\tau_n} \right) \langle \delta x \xi \rangle + \langle \xi^2 \rangle \tag{S41}$$

$$\langle \dot{\xi^2} \rangle = -\frac{2}{\tau_n} \langle \xi^2 \rangle + \frac{2\sigma^2}{\tau_n}. \tag{S42}$$

The steady state solutions are

$$\langle \xi^2 \rangle_* = \sigma^2 \tag{S43}$$

$$\langle \delta x \xi \rangle_* = \frac{\sigma^2}{\frac{1}{\tau_n} - \lambda} \tag{S44}$$

$$\langle \delta x^2 \rangle_* = V_{eq} = \frac{\sigma^2}{\lambda(\lambda - \frac{1}{\tau_n})}. \tag{S45}$$

To get the full solution for the variance, we will simplify by assuming that $\langle \xi^2 \rangle$ and $\langle \delta x \xi \rangle$ are in equilibrium and insert their steady state solutions into the equation for the variance Eq. (S40)

$$\frac{dV}{dt} = 2\lambda(t)V(t) + 2\frac{\sigma^2}{\frac{1}{\tau_n} - \lambda}. \tag{S46}$$

The denominator in the second term, which is now time dependent, is determined by the interplay between the correlation time of the noise $\tau_n$ and the relaxation rate of the system

$$\frac{1}{\tau_n} - \frac{1}{2\tau_s}(1 - 3x_{det}^2) \equiv \frac{1}{\tau_n} + \frac{1}{\tau(t)}. \tag{S47}$$

where we introduced the current time scale of the system, $\tau(t)$, as the negative reciprocal of $\lambda(t)$. The second term will always be bounded by the values of the relaxation rate. In our model, $x \in [-1, \sim 1.2]$ (the range spanned during the ramp-up of the forcing parameter). This will also hold for dimensional systems, since the meaningful variable here is $x/x_0$, where $x_0$ is the natural scale of the system. The relaxation rate is thus restricted to $|\lambda| \lesssim 1/\tau_s$. This

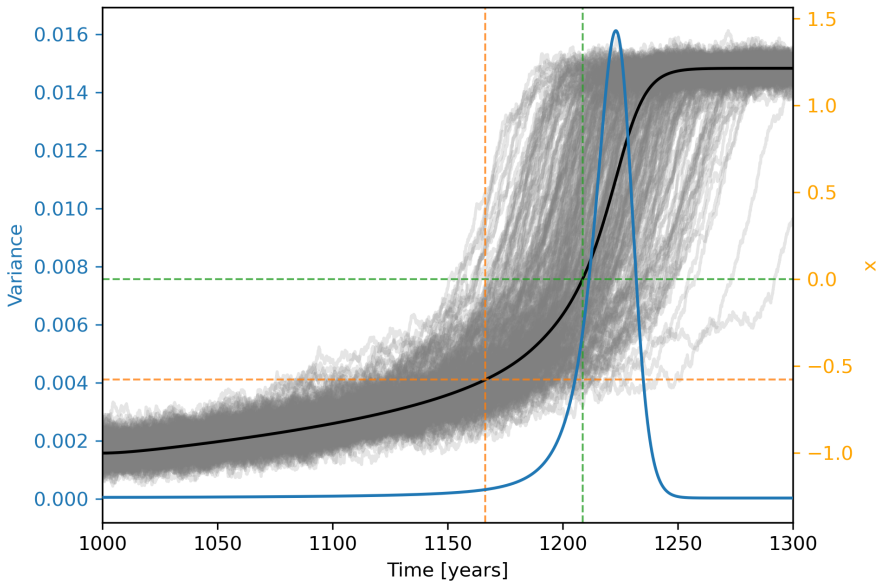
means that the variance injection term depends entirely on the ratio between the noise time scale $\tau_n$ and the system time scale $\tau$. For our system, in which the noise correlation time is around 10 days, whereas the system time scale ranges between 1-10 years $1/\tau_n \gg 1/\tau_s$ will always hold. We can therefore neglect the second term in the denominator and obtain

$$\frac{dV}{dt} = 2\lambda(t)V(t) + 2\sigma^2\tau_n. \tag{S48}$$

The time evolution of variance in our system can thus be described by the variance equation for white noise Eq. (S21) with variance injection depending on the correlation time of the noise $\tau_n$. Analogously to Eq. (S27) this then yields the solution

$$V(t) = V(t_0)e^{\int_{t_0}^{t} 2\lambda(u)du} + 2\sigma^2\tau_n \int_{t_0}^{t} e^{\int_{s}^{t} 2\lambda(u)du} ds. \tag{S49}$$

In Fig. 1, this solution together with the ensemble of stochastic runs is shown for $\tau = 10\,\mathrm{yr}$. This visualises that the maximum of the variance is located at the time at which the spread in trajectories compared to the deterministic trajectory is largest. Before and after the maximum, a significant amount of trajectories are in the old or new equilibrium state, reducing the spread. Note that the maximum in this system is reached significantly after the tipping point and even after the point of no return of the deterministic trajectory. We now have an analytical tool to determine the uncertainty along the trajectory of a system going through a tipping process.




**Supplementary Figure 1**: Solution of variance equation for $\tau = 10\,\mathrm{yr}$, $\tau_f = 125\,\mathrm{yr}$ and $\tau_n = 10\,\mathrm{days}$ together with ensemble of stochastic trajectories and deterministic solution $x_{det}$. The variance has a maximum where the spread of trajectories is highest.

## Supplementary Note 4: Variance decomposition

In order to get an analytical expression that is comparable to the fluctuation variance that we measure numerically with our detrending method, we will decompose the variance such that we get a part that is calculated over the trajectories that are aligned along the POR, as in Fig. 1 of the main script. In order to do so we have to introduce the index $i$ that numerates the individual runs in the ensemble. For each trajectory there is a separate crossing time $t^i_{POR}$ of the POR

$$x^i(t^i_{POR}) = 0. \tag{S50}$$

We can expand the time of the POR crossing around the deterministic crossing time $t_{POR}$

$$t^i_{POR} = t_{POR} + \delta t^i. \tag{S51}$$

This yields

$$0 = x^i(t^i_{POR}) \approx x^i(t_{POR}) + \dot{x}^i(t_{POR})\delta t^i. \tag{S52}$$

Also expanding $\dot{x}^i(t_{POR})$ around the deterministic trajectory and only keeping first order terms we obtain

$$0 = \delta x^i(t_{POR}) + \dot{x}_{det}(t_{POR})\delta t^i. \tag{S53}$$

Solving for $\delta t^i$ and taking the variance on both sides we obtain an expression for how much the POR time varies across runs

$$\delta t^i = -\frac{\delta x^i(t_{POR})}{\dot{x}_{det}(t_{POR})} \Leftrightarrow V(\delta t) = \frac{V(t_{POR})}{\dot{x}_{det}(t_{POR})^2}. \tag{S54}$$

This will be useful later. We now introduce the relative time $\tilde{t}$ and define the ensemble of aligned trajectories

$$X_a^i(\tilde{t}) = x^i(t_{POR} + \tilde{t} + \delta t^i) \approx x_{det}(t_{POR} + \tilde{t}) + \delta x^i(t_{POR} + \tilde{t}) + \dot{x}_{det}(t_{POR} + \tilde{t})\delta t^i \tag{S55}$$

where we used the same first order velocity expansion as in Eq. (S53). We now define the deviation of the stochastic runs from the deterministic solution at time $\tilde{t}$

$$\Delta x^i(\tilde{t}) \equiv X_a^i(\tilde{t}) - x_{det}(t_{POR} + \tilde{t}). \tag{S56}$$

Inserting Eq. (S55) yields

$$\Delta x^i(\tilde{t}) \approx \delta x^i(t_{POR} + \tilde{t}) + \dot{x}_{det}(t_{POR} + \tilde{t})\delta t^i \tag{S57}$$

Since $\Delta x^i(\tilde{t})$ and the aligned trajectories $X_a^i(\tilde{t})$ only deviate from each other by the deterministic trajectory, which is the same for all realisations, (Eq. (S56)) we can write

$$V(X_a) \equiv V_a(\tilde{t}) = V(\Delta x) = \mathrm{E}[\Delta x^i(\tilde{t})^2] \tag{S58}$$

where the last equivalence follows from the mean of $\Delta x$ being 0. Inserting Eq. (S57) we obtain

$$V_a(\tilde{t}) = \mathrm{E}[\delta x(t_{POR} + \tilde{t})^2] + \dot{x}_{det}(t_{POR} + \tilde{t})^2\mathrm{E}[\delta t^2] + 2\dot{x}_{det}(t_{POR} + \tilde{t})\mathrm{E}[\delta x(t_{POR} + \tilde{t})\delta t]. \tag{S59}$$

Defining the covariance as

$$\mathrm{Cov}(\delta x^i(t_{POR}), \delta x^i(t)) \equiv C(t) \tag{S60}$$

and inserting Eq. (S54) yields

$$V_a(\tilde{t}) = V(t_{POR} + \tilde{t}) + r(\tilde{t})^2 V(t_{POR}) - 2r(\tilde{t})C(t_{POR} + \tilde{t}) \tag{S61}$$

where we defined

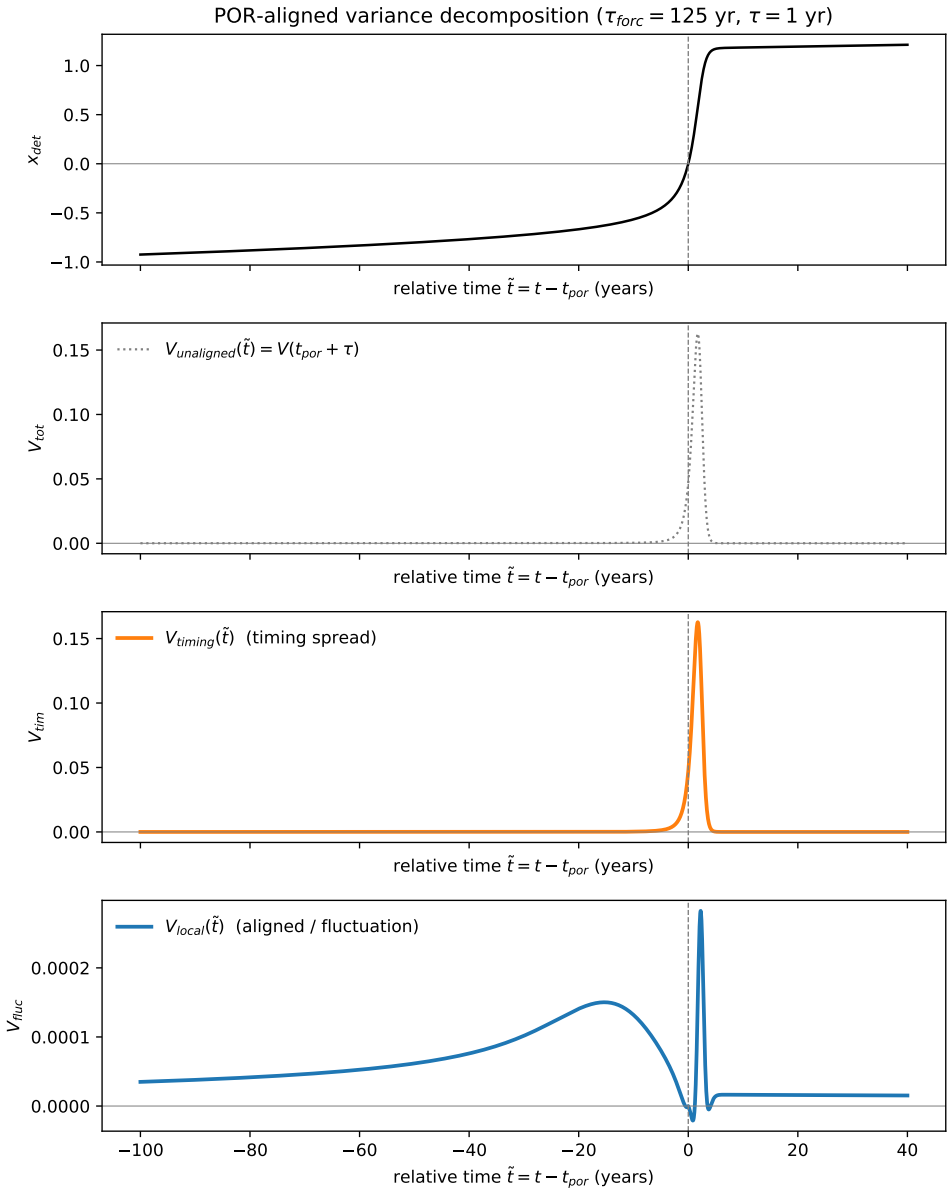
$$r(\tilde{t}) \equiv \frac{\dot{x}_{det}(t_{POR}+\tilde{t})}{\dot{x}_{det}(t_{POR})}. \tag{S62}$$

Within the linearisation, the covariance is $C(t) = V(t_{POR})\exp(\int_{t_{POR}}^{t}\lambda(u)du)$ for $t \geq t_{POR}$ and $C(t) = V(t)\exp(\int_{t}^{t_{POR}}\lambda(u)du)$ for $t < t_{POR}$. This is now an expression for the aligned variance. The first term in Eq. (S61) describes the original, unaligned variance, the second term only the variance caused by differing timing/trajectory deviations and the third term the covariance between the two.

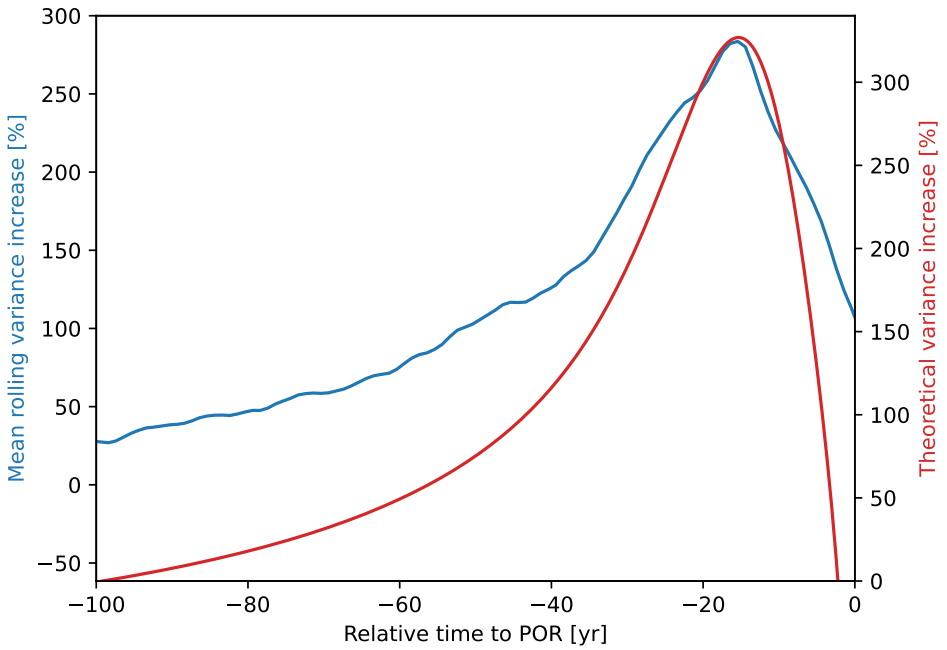
Fig. 2 illustrates the decomposition of Eq. (S61) for $\tau_{forc} = 125\,\text{yr}$, $\tau_s = 1\,\text{yr}$. The top panel shows the deterministic trajectory $x_{det}(t)$, plotted against relative time $\tilde{t} = t - t_{POR}$, so that the point of no return coincides with $\tilde{t} = 0$. The second panel shows $V_{unaligned}(\tilde{t}) \equiv V(t_{POR} + \tilde{t})$, the original (unaligned) variance solution re-indexed onto relative time. This quantity mixes fluctuation-driven and timing-driven spread and is sharply peaked around $\tilde{t} = 0$, where the ensemble spread is dominated by the fact that different realisations cross the POR at different times. The third panel shows $V_{timing}(\tilde{t}) \equiv 2r(\tilde{t})C(t_{POR}+\tilde{t}) - r(\tilde{t})^2 V(t_{POR})$, the part of the variance attributable to this timing spread, reprojected into $x$-space by multiplying with the local slope of the deterministic trajectory. The bottom panel shows $V_a(\tilde{t})$ (Eq. (S61)), the aligned variance obtained after subtracting the timing contribution from $V_{unaligned}$. By construction $V_a(0) = 0$, since every realisation sits exactly at $x = 0$ at its own crossing time. Away from $\tilde{t} = 0$, $V_a(\tilde{t})$ is intended to isolate the variance caused by fluctuations around the mean state of a trajectory, as opposed to the variance caused by uncertainty in the trajectory's timing.

Interpreting $V_a$ as a fluctuation variance requires that deviations between nearby realisations are damped rather than amplified. This is the case when the relaxation rate $\lambda$ is negative, i.e. for $|x_{det}| > |x_c|$. This hold throughout the pre-tipping branch, before the tipping point is reached and $\lambda$ becomes 0.

Beyond that point for $x_{det} \in (x_c, -x_c)$ we have $\lambda(t) > 0$, and nearby realisations no longer contract onto a common trajectory but genuinely diverge from one another in their shape. In this regime, individual realisations can differ in the overall shape of their evolution, not only in timing, so a single scalar offset $\delta t^i$ can no longer capture how they differ. As a consequence, "variance due to fluctuations around the mean state" and "variance due to differing trajectory evolution" are no longer separable. We therefore restrict the comparison between the mean rolling (detrended) variance and the analytic aligned variance $V_a(\tilde{t})$ to $x_{det}(t) < x_c$. Within this range the two independently obtained estimates of the fluctuation variance agree well in both the location and the height of their peak for $\tau_s = 1\,\text{yr}$ (Fig. 3).




**Supplementary Figure 2**: Decomposition of the ensemble variance into timing and fluctuation contributions for $\tau_{forc} = 125\,\text{yr}$ and $\tau_s = 1\,\text{yr}$, plotted against the time relative to the deterministic crossing of the point of no return. (a) Deterministic trajectory. (b) Unaligned variance from the linear variance equation, containing both the spread due to differing crossing times and the fluctuations around the mean state. (c) Timing contribution, i.e. the part of the variance explained by the spread in crossing times. (d) Aligned variance after subtracting the timing contribution, which vanishes at the point of no return by construction.




**Supplementary Figure 3**: Comparison of the fluctuation variance obtained from the stochastic ensemble and from the analytic decomposition for $\tau_{forc} = 125\,\text{yr}$ and $\tau_s = 1\,\text{yr}$. Shown are the ensemble mean of the rolling variance of the detrended runs (Fig. 1a in the main text) and the analytically aligned variance up to the POR.

## Supplementary Note 5: Non-dimensionalization with red noise

Consider the original system

$$\frac{dx}{dt} = \frac{x_0}{2\tau_s}\left(-\left(\frac{x}{x_0}\right)^3 + \left(\frac{x}{x_0}\right) + \theta(t)\right) + \xi(t) \tag{S63}$$

$$\frac{d\xi}{dt} = -\frac{\xi}{\tau_n} + \sqrt{\frac{2\sigma^2}{\tau_n}}\,\eta(t) \tag{S64}$$

$$\theta(t) = \frac{t}{\tau_f} \tag{S65}$$

where $\eta(t)$ is white noise.

Using the scales $x_0$ for $x$ and $\tau_n$ for $t$, we define the non-dimensionalize variables

$$\bar{x} \equiv \frac{x}{x_0}, \qquad \bar{t} \equiv \frac{t}{\tau_n}, \qquad \bar{\xi} \equiv \frac{\xi}{\left(\frac{x_0}{\tau_n}\right)}. \tag{S66}$$

which yields with the non-dimensional parameters

$$\bar{\sigma}^2 \equiv \frac{\tau_n^2}{x_0^2}\,\sigma^2, \qquad \bar{\tau}_s \equiv \frac{\tau_s}{\tau_n}, \qquad \bar{\tau}_f \equiv \frac{\tau_f}{\tau_n}. \tag{S67}$$

and the normalized white noise $\bar{\eta} \equiv \sqrt{\tau_n} \cdot \eta$ the non-dimensional set of equations

$$\frac{d\bar{x}}{d\bar{t}} = \frac{1}{2\bar{\tau}_s}\left(-\bar{x}^3 + \bar{x} + \bar{\theta}\right) + \bar{\xi} \tag{S68}$$

$$\frac{d\bar{\xi}}{d\bar{t}} = -\bar{\xi} + \sqrt{2\bar{\sigma}^2}\,\bar{\eta} \tag{S69}$$

$$\bar{\theta} = \frac{\bar{t}}{\bar{\tau}_f} \tag{S70}$$

## References


[1] Lenton, T. M. *et al.* Tipping elements in the earth's climate system. *Proceedings of the National Academy of Sciences* **105**, 1786–1793 (2008).

[2] Levermann, A. *et al.* Potential climatic transitions with profound impact on europe: Review of the current state of six 'tipping elements of the climate system'. *Climatic Change* **110**, 845–878 (2012).

[3] Armstrong McKay, D. I. *et al.* Exceeding 1.5°c global warming could trigger multiple climate tipping points. *Science* **377**, eabn7950 (2022).

[4] Stommel, H. Thermohaline convection with two stable regimes of flow. *Tellus* **13**, 224–230 (1961).

[5] Levermann, A. & Born, A. Bistability of the Atlantic subpolar gyre in a coarse-resolution climate model. *Geophysical Research Letters* **34**, L24605 (2007).

[6] Born, A. & Stocker, T. F. Two stable equilibria of the Atlantic subpolar gyre. *Journal of Physical Oceanography* **44**, 246–264 (2014).

[7] Zickfeld, K., Knopf, B., Petoukhov, V. & Schellnhuber, H. J. Is the Indian summer monsoon stable against global change? *Geophysical Research Letters* **32**, L15707 (2005).

[8] Brovkin, V., Claussen, M., Petoukhov, V. & Ganopolski, A. On the stability of the atmosphere-vegetation system in the Sahara/Sahel region. *Journal of Geophysical Research: Atmospheres* **103**, 31613–31624 (1998).

[9] Schoof, C. Ice sheet grounding line dynamics: Steady states, stability, and hysteresis. *Journal of Geophysical Research: Earth Surface* **112**, F03S28 (2007).

[10] Weertman, J. Stability of the junction of an ice sheet and an ice shelf. *Journal of Glaciology* **13**, 3–11 (1974).

[11] North, G. R. The small ice cap instability in diffusive climate models. *Journal of the Atmospheric Sciences* **41**, 3390–3395 (1984).

[12] Eisenman, I. & Wettlaufer, J. S. Nonlinear threshold behavior during the loss of arctic sea ice. *Proceedings of the National Academy of Sciences* **106**, 28–32 (2009).

[13] Levermann, A. & Winkelmann, R. A simple equation for the melt elevation feedback of ice sheets. *The Cryosphere* **10**, 1799–1807 (2016). URL http://www.the-cryosphere.net/10/1799/2016/.

[14] Robinson, A., Calov, R. & Ganopolski, A. Multistability and critical thresholds of the greenland ice sheet. *Nature Climate Change* **2**, 429–432 (2012). URL https://doi.org/10.1038/nclimate1449.

[15] Staver, A. C., Archibald, S. & Levin, S. A. The global extent and determinants of savanna and forest as alternative biome states. *Science* **334**, 230–232 (2011).

[16] Scheffer, M., Hirota, M., Holmgren, M., Van Nes, E. H. & Chapin, F. S. Thresholds for boreal biome transitions. *Proceedings of the National Academy of Sciences* **109**, 21384–21389 (2012).

[17] Garbe, J., Albrecht, T., Levermann, A., Donges, J. F. & Winkelmann, R. The hysteresis of the Antarctic Ice Sheet. *Nature* **585**, 538–544 (2020).

[18] Jin, F.-F. An equatorial ocean recharge paradigm for ENSO. part I: Conceptual model. *Journal of the Atmospheric Sciences* **54**, 811–829 (1997).

[19] Ashwin, P., Wieczorek, S., Vitolo, R. & Cox, P. Tipping points in open systems: bifurcation, noise-induced and rate-dependent examples in the climate system. *Philosophical Transactions of the Royal Society A* **370**, 1166–1184 (2012).